

Equation of State of He³ Close to the Critical Point*

Barrie Wallace, Jr., and Horst Meyer

Department of Physics, Duke University, Durham, North Carolina 27706

(Received 2 March 1970)

We present measurements of the equation of state of He³ with an impurity of 250 ppm He⁴ near the critical point. In these experiments the density is measured by a dielectric-constant technique. The density cell is a horizontal capacitor to reduce the gravitational effects. The temperature gradient between the cell and 4°K occurs along a horizontal capillary. The results are analyzed in terms of the critical exponents which are found to have values similar to those of other simple fluids. From the coexistence curve and the compressibility on the critical isochore above T_c , we get $\beta = 0.361$, $B = 1.31$, $\gamma = 1.18$, $\Gamma = 2.48 \times 10^{-4} \text{ Torr}^{-1}$, $T_c = 3.3105 \text{ }^\circ\text{K}$, $\rho_c = 0.04145 \text{ g/cm}^3$, and $P_c = 860.5 \text{ Torr}$. From the compressibility along the coexistence curve, we obtain $\gamma' = 1.12$ and $\Gamma' = 6.9 \times 10^{-5} \text{ Torr}^{-1}$ for both the liquid and the vapor sides. An analysis of the critical isotherm using the conjugate variables μ and ρ gives $\delta = 4.21 \pm 0.10$ and $\nabla = 2.77$. The critical isobar gives the exponents $\pi_+(\rho > \rho_c) = 4.21 \pm 0.10$ and $\pi_-(\rho < \rho_c) = 4.35 \pm 0.10$. The study of the critical isochore shows d^2P/dT^2 to be always positive. Combination of these data with specific-heat results by Moldover indicate no discontinuity in $d^2\mu/dT^2$ within experimental error. We find at the critical point $(P_c V_c)^{-1} d^2\mu/dT^2 = -0.22 \text{ (}^\circ\text{K)}^{-2}$. The isotherms expressed by the conjugate variables μ, ρ are fitted to the scaling equation of state proposed by Missoni *et al.* A good fit was obtained with the following parameters: $E_1 = 2.53$, $E_2 = 0.44$, $\delta = 4.23$, $x_0 = 0.475$, and $\gamma = 1.17$. Results of a less extensive study of He³ with an impurity of 10 ppm are presented. They give critical indices and P_c , T_c , and ρ_c in substantial agreement with the less pure He³. A comparison of the present data with previous work is presented.

I. INTRODUCTION

Recently much research, several review papers, and a number of conferences have focussed attention on the behavior of fluids and magnetic materials near the critical point, which separates the inhomogeneous two-phase region from the homogeneous one-phase region.¹⁻³ Description of fluids by means of the scaling ideas has been discussed most recently by Missoni^{4,5} and by Schofield *et al.*⁶ Attention was paid in particular to the properties of CO₂, Xe, and He⁴, for which good measurements are available.

The research described below is concerned with the equation of state of He³ in the neighborhood of the critical point. This research constitutes an improvement and extension of previous work in this laboratory.⁷ Recent research on He³ in other institutions includes that by Kerr and Sherman,⁸ Chase and Zimmerman,⁹ Moldover and Little^{10,11} as well as previous work by them.¹²⁻¹⁴

From our work, which comprises the measurement of the density along isotherms and isobars and also the pressure versus temperature along the critical isochore, we present a discussion of the validity of the scaling ideas using the closed form of the chemical potential μ proposed by Missoni *et al.*^{4,5} A fit of the data to the linear model of the parametric equation of state⁶ has been made by Ho and Litster and will be presented elsewhere.¹⁵

We find that the experimental results can be well represented by this theory for densities ρ such that $|\rho - \rho_c|/\rho_c \leq 0.25$. In another paper we will discuss the critical isotherm outside this density range and compare it with the expectations for an "asymmetric lattice gas".¹⁶

II. BRIEF REVIEW OF SCALING RELATIONS

For the convenience of the reader, we list below some of the relations used to describe the critical singularities, where we adopt the notation found in previous work,¹⁷ extended to isobars and where

$$\Delta P = [P(\rho, T) - P(\rho_c, T)]/P_c, \quad (1)$$

$$\Delta \rho = [\rho(T, P) - \rho_c]/\rho_c, \quad (2)$$

$$t = (T - T_c)/T_c. \quad (3)$$

We use the variable conjugates μ (chemical potential) and ρ for the isotherms, since it was shown by Missoni *et al.*^{4,5} that these are the most suitable in terms of symmetry arguments for discussing thermodynamic properties in the region of the critical point. One obtains the following equations for cases (a)-(g): (a) coexistence curve

$$\Delta \rho = (\rho_c - \rho_c)/\rho_c \simeq (\rho_L - \rho_c)/\rho_c \simeq B(-t)^\delta, \quad (4)$$

where ρ_c and ρ_L are, respectively, the density of the vapor and liquid along the coexistence curve; (b) critical isotherm

$$\Delta P \propto [\mu(\rho, T_c) - \mu(\rho_c, T_c)]/P_c V_c = \nabla \Delta\rho |\Delta\rho|^{\delta-1}; \quad (5)$$

(c) critical isobar

$$t = \Pi \Delta\rho |\Delta\rho|^{\pi-1}; \quad (6)$$

(d) compressibility on the critical isochore

$$k_T = \Gamma_T t^{-\gamma_T}, \quad T > T_c; \quad (7)$$

(e) thermal expansion on the critical isochore

$$\rho_c^2 \left(\frac{1}{\rho} \left(\frac{\partial \rho}{\partial T} \right)_P \right) \approx \Gamma_P t^{-\gamma_P}, \quad T > T_c; \quad (8)$$

(f) compressibility along the coexistence curve in the one-phase region

$$(\rho/\rho_c)^2 k_T \approx \Gamma'_T (-t)^{-\gamma'_T}, \quad T < T_c; \quad (9)$$

(g) specific heat at constant volume on the critical isochore

$$C_V \approx \frac{A^+}{\alpha} t^{-\alpha} + D^+, \quad T > T_c, \quad (10)$$

$$C_V \approx \frac{A^-}{\alpha} (-t)^{-\alpha'} + D^-, \quad T < T_c. \quad (11)$$

The critical indices are connected by various thermodynamic relations. Griffiths,^{18,19} Rushbrooke,²⁰ and Fisher¹⁷ have derived inequalities that must be satisfied if the power-law assumptions are to provide an adequate description of the singularities at the critical point:

$$\beta(\delta + 1) + \alpha' \geq 2, \quad (12)$$

$$\gamma'_T(\delta + 1)/(\delta - 1) + \alpha' \geq 2, \quad (13)$$

$$\gamma'_T + 2\beta + \alpha' \geq 2. \quad (14)$$

A useful check on the internal consistency of the data would be to treat Eqs. (12) and (14) as equalities, in which case one obtains the relation

$$\beta(\delta - 1) = \gamma'_T. \quad (15)$$

Using reasonable hypotheses (in particular, the assumption that $d^2P/dT^2 \geq 0$ for the vapor pressure curve near T_c , which we later show to be verified for He³) Griffiths¹⁸ has shown that for $\rho > \rho_c$, i. e., on the liquid side of the critical point, π should be the same as δ . The situation on the vapor side is not clear at present, and the reader is referred to the discussion by Griffiths.¹⁸ However, it appears from the experiments on He³ that the difference between π and δ on the vapor side is only marginal. We also note the equality (by definition) relating the compressibility and thermal expansion coefficients both above and below T_c :

$$\frac{1}{\rho} \left(\frac{\partial \rho}{\partial T} \right)_P = \left(\frac{\partial P}{\partial T} \right)_V k_T. \quad (16)$$

Following the ideas of Griffiths,³ Missoni *et al.*^{4,5} have used the variable

$$x = t/|\Delta\rho|^{1/\beta} \quad (17)$$

and have proposed and discussed a closed-form approximation for the equation of state:

$$\Delta\mu = \mu(\rho, t) - \mu(\rho_c, t) = \Delta\rho |\Delta\rho|^{\delta-1} h(x). \quad (18)$$

From the general properties of such a function³ $h(x)$, as determined by the requirement of analyticity of the thermodynamic potentials, it follows that

$$\gamma_T = \beta(\delta - 1) = \gamma'_T. \quad (19)$$

Based on various requirements, Missoni *et al.* assumed the function

$$h(x) = E_1 \left(\frac{x+x_0}{x_0} \right) \left[1 + E_2 \left(\frac{x+x_0}{x_0} \right)^{2\beta} \right]^{(\gamma_T-1)/2\beta}. \quad (20)$$

For $x = -x_0 = B^{-1/\beta}$, we find $h(x) = 0$. Although $h(x=0)$ is nonanalytic at this point, its derivative $h'(-x_0) = E_1$ is finite, which means that the compressibility on the phase boundary is finite and behaves like $(-t)^{-\gamma_T}$, as has been pointed out by Missoni *et al.*⁵

The constants E_1 , E_2 , x_0 , β , and γ_T are to be determined from the experiments. Although this number of constants is large, some of these (x_0 and β) can be determined independently from the precise measurement of the coexistence curve, or (as for γ_T) from the critical isochore above T_c . As we shall see, the large amount of data provides a good check of the internal consistency of these constants.

III. EXPERIMENTAL

The experiment consisted in measuring the density of a sample of He³ with 250 ppm He⁴ by means of a capacitive technique. The sample serves as the dielectric medium between the plates of a capacitor and determines the dielectric coefficient via the Clausius-Mosotti relation:

$$\frac{\epsilon - 1}{\epsilon + 2} = \frac{4\pi}{3M} \rho \alpha, \quad (21)$$

where α is the polarizability and M is the molecular mass of He³. The polarizability is assumed to be constant and equal to 0.1234 cm³/mole.⁸ Although the very precise measurements of Kerr and Sherman⁸ have shown that there is, in fact, a small variation of α with density, the correction to the experimental data (Sec. V) is small and comparable with the uncertainty of the experiment. This will be discussed below.

The density cell for the measurements with 250 ppm He⁴ is shown schematically in Fig. 1. In order to reduce the effects of gravity, which have been discussed by several authors and most recently by Buckingham,²¹ the cell is essentially a horizontal-plate capacitor. The two parts forming the capacitor are of electrolytic copper and are

electrically isolated from one another by means of Mylar spacers of 0.0025 cm thickness. These parts are cemented together by Stycast epoxy material. The cross-sectional area of the capacitor is approximately 1.6 cm². The inner diameter of the fill capillary is 0.5 mm, which determines the minimum height of the assembly. The effective height of He³ in the cell is unlikely to be more than about 1.5 mm, based on the space taken by the epoxy. It is estimated that about 90% of the sample is situated within a height of 0.5 mm. Any additional height due to possible tilt is negligible.

The measurements with the 10-ppm-He⁴ sample were carried out with a cell of slightly different design to test the effect of the cell height. This new cell had a cross-sectional area of 2 cm²; the fill capillary had an inner diameter of 0.4 mm. Extra careful horizontal positioning of the cell and improvement of the design gave then an effective height of less than 0.5 mm. The times required to reach equilibrium were not different from those with the first cell. The results obtained (Sec. VI) lead us to believe that the two cells gave consistent results and that gravity effects were negligible.

To avoid any change of the hydrostatic pressure from the column of He³ leading to the cell, the temperature gradient between the 4.2 °K bath and the cell was made horizontal. This was accomplished by using thick copper wires to thermally anchor the He³ filling capillary to the 4.2 °K bath at the height of the sample capacitor. The cell was made part of the tank circuit of a tunnel diode oscillator,²² the frequency of which was measured by means of an electronic counter, as described previously. The stability of this oscillator was about ± 2 Hz per day while the frequency ν was of the order of 14 MHz. This stability made it possible in principle to reproduce the density within a day and under identical conditions to within about $2 \times 10^{-4}\%$. The dielectric constant of the sample is related to the frequency as²²

$$\epsilon = \frac{(\nu_0/\nu)^2 + C[(\nu_0/\nu)^2 - 1]}{1 + BP}, \quad (22)$$

where ν_0 is the frequency of the empty capacitor, BP is a correction for the distortion of the capacitor as the pressure changes, and C is a term due to the capacity of the condenser part filled with Stycast and to various other parts in the circuit. The procedure of calibration is described below.

The temperature of the sample was determined from a Cryocal germanium resistor thermally bonded to the capacitor, and used in a two-lead arrangement with a 200-Hz Wheatstone bridge. To compensate for temperature effects from the lead resistance, an identical pair of leads, also mounted in the cryostat and subjected to the same tempera-

ture profile, was connected electrically in series with the standard resistor decade boxes. The sensitivity of the bridge was such that temperature changes of 5 μ K near 3.3 °K could be resolved. The phase-sensitive detector of the bridge was connected to a heater circuit making possible the temperature regulation of the sample capacitor. Temperature stabilities to within 20 μ K were then achieved for the various isotherms.

The sample pressure was measured by a Texas Instruments fused Quartz Bourdon gauge that had a stated resolution of 0.025 Torr. This gauge was initially calibrated against a mercury manometer and periodically checked against it for possible drifts. The pressure in the system was controlled by means of the variable volume of a finely adjustable piston which allowed very small changes in P to be made conveniently.

IV. CALIBRATION PROCEDURES AND EXPERIMENTAL ERRORS

A. Thermometry

Approximately 40 measurements of the germanium thermometer resistance R were taken in the interval 2.9–3.8 °K by reading the vapor pressure of He⁴ in the pot of Fig. 1 from the height of a mercury manometer. The necessary corrections were made to convert to readings taken under standard conditions. The external helium bath was regulated to a temperature only slightly above that of the pot, so that there was only a very small

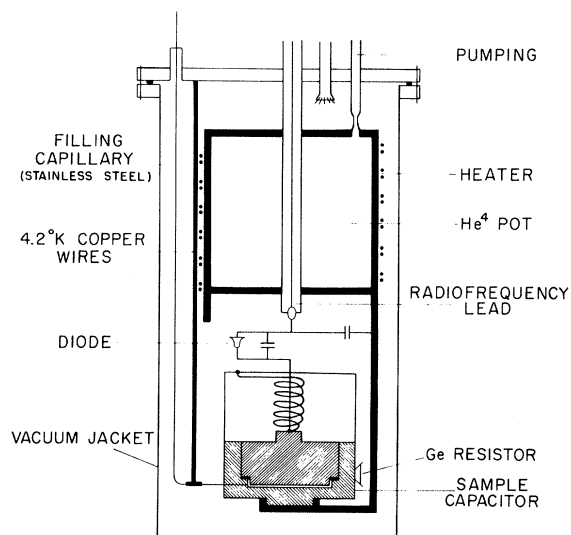


FIG. 1. Schematic presentation of the cryostat, including the density cell. The vacuum jacket is surrounded by liquid He⁴, usually kept at 4.2°K, except during the thermometer calibration.

temperature gradient and the temperature drift with time of the pot was negligible. The vapor pressure was related to the absolute temperature by means of the 1958 He⁴ vapor-pressure scale.²³ A least-squares-fit technique was applied to the equation

$$\log (T - F) = C_1 \log R + C_2, \quad (23)$$

where F was determined by iteration. The deviations between the measurements and the curve so obtained were random and gave a mean-square temperature deviation of 0.3 mK. We estimate that accuracy of our temperature scale to be within 0.5 mK of the 1958 scale. The temperature calibration was not subjected to the same uncertainties as those discussed by Missoni for the work on He⁴.²⁴

B. Capacitor

At the beginning of an experiment, after a thorough check on the stability of the oscillator, the frequency ν_0 of the empty sample capacitor was measured as a function of temperature and the resulting set of points was fitted with a polynomial $\sum_{i=-2}^{i=+2} a_i T^i$ with a random deviation of ± 1 Hz. Immediately after admitting He³ into the capacitor, a calibration at $T = 2.9$ °K of frequency ν versus P in the liquid phase was carried out. Data of the density at this temperature and pressure were taken from results obtained with another capacitor.²⁵ This latter cell, calibrated with He⁴ from pycnometric measurements,²⁶ had given results for He³ that were approximately $0.15 \pm 0.1\%$ lower than those at 1.0 atm obtained by Sherman and Edeskuty.²⁷

In our calibration, we have made the reasonable assumption that the constants C and B are temperature independent in the region 3.8–2.5 °K. We found $B = -1.828 \times 10^{-4} \text{ atm}^{-1}$, which is of the same order as that for the previous density cell.²⁵

Because of the refilling of the He⁴ pot every two days and the transfer of liquid helium into the main bath, there were some unavoidable, small frequency shifts. These were taken into account by a daily recalibration of the frequency versus pressure at 2.9 °K and a corresponding shift, when necessary, was applied to the ν_0 -versus- T curve.

Based on considerations of the long-term stability, and on possible systematic uncertainties in our calibration, as well as those due to the slight density dependence of the polarizability, we estimate the uncertainty in our *absolute* value of the density to be approximately 0.5% at the critical density, while the density resolution, as mentioned before, is much better, being $\delta\rho/\rho_c \approx 5 \times 10^{-3}\%$ near ρ_c . Because of the difficulties inherent in the experiment, a density at a given T and P , as read by the

resistance bridge and the quartz gauge in the course of a long experiment, could only be reproduced to about $5 \times 10^{-2}\%$.

C. Pressure Measurement

As mentioned before, the calibration of the Quartz gauge was regularly checked against the height of a mercury column. This height, corrected to standard conditions, was determined to ± 0.1 Torr. The shifts of the calibration curve were of the order of 0.2 Torr over periods of days, in a random way. We thus estimate the accuracy of the pressure reading to be about ± 0.2 Torr compared with resolution of the instrument, which is 0.025 Torr. The pressure difference $P(4 \text{ °K}) - P(300 \text{ °K})$ between room temperature and the cell was calculated to be about $5 \times 10^{-4} P$, assuming the ideal-gas law to hold and taking a realistic temperature profile in the cryostat. This systematic correction, although it increases the absolute value of P near the critical point by about 0.5 Torr, is too small to affect significantly the calculation of the quantities of interest such as ΔP and $\Delta\mu$ and has not been incorporated into the tabulated results, except for the tabulated P_c .

D. Experimental Procedure

Isotherm data were taken by changing the amount of sample in the system by means of the movable piston and waiting for the frequency ν and the pressure P to reach equilibrium. The time τ that elapsed between two data points was usually of the order of 10–15 min even in close proximity of the critical point. In half of that time P and ν had reached an equilibrium value, which was then closely monitored for the remaining 5 min. Hence the data taking was considerably shorter than it was with the density cell having a height of 1 cm and for which τ could attain 1 or 2 h very close to T_c .⁷ The isobars, obtained by changing the temperature and manually keeping the pressure constant, took about 20 min per point, because of the more tedious manipulations. Once the critical density was determined from an analysis of the isotherms and isobars, the critical isochore was taken by changing the pressure and temperature in such a way that the frequency stayed constant at the value ν_c computed for the density ρ_c .

V. RESULTS AND DISCUSSION

Because of the large amount of data taken, both on isotherms and isobars, that extends over a region of $-0.1 < t < 0.05$ and $|\Delta\rho| \lesssim 0.5$, a tabulation appears impractical in this paper and is being submitted to the National Auxiliary Publications Service, sponsored by the American Society for Information Science. These tables are also available in

computer sheet format from the authors. Here we merely list, in Table I, the temperatures and pressures at which the isotherms and isobars were taken. A systematic check for internal consistency was made between both sets of data. For a given P and T , the densities were found to be equal to within 0.1%. We have also obtained (by numerically integrating the isotherms) the normalized chemical potential $\Delta\mu/P_c V_c = \int V dP/P_c V_c$. (Tabulations are also available upon request.) We now describe the various steps in the analysis.

A. Properties on the Coexistence Curve; Compressibility and Thermal Expansion along the Critical Isochore

The coexistence data obtained from 18 isotherms and isobars and gave ρ_G and ρ_L as a function of T (Table I). The average value $\bar{\rho} = \frac{1}{2}(\rho_G + \rho_L)$ did not change significantly in the temperature range investigated, being 0.04145 g/cm³. We add that the limiting value at $T=0$ is not very different, being $\bar{\rho}(T=0) = \frac{1}{2}\rho_L(T=0) = 0.0405$ g/cm³, where $\rho_L(T \approx 0)$ has been taken from the work of Kerr and Taylor.^{28,29} For temperatures above T_c , the inflection density ρ_{inf1} in the μ, ρ plane for a given isotherm was determined from the maximum in a plot of $\partial\rho/\partial\mu = \rho^2 k_T = \rho(\partial\rho/\partial P)_T$ versus ρ . The ρ_{inf1} values so obtained were found to be very close to $\bar{\rho}$ and were taken to be equal to ρ_c . The maximum

of k_T for a given isotherm occurs, of course, at a density $\rho < \rho_{\text{inf1}}$. For a discussion of this point, see the paper by Widom.³⁰ The inflection density for a given isobar was obtained from the maximum of a plot of $1/\rho(\partial\rho/\partial T)_P$ versus ρ . It was also found to be very close to $\bar{\rho}$. Table I gives the experimental values for ρ_{inf1} both for isotherms and isobars. The critical temperature T_c was then located from the data of Table I and from $\rho_c^2 k_T(T > T_c)$ using a least-squares fit to Eqs. (4) and (7), where the parameters to be determined were B , β , Γ , γ , and T_c . The temperature range over which the fit was made was $0.001 \lesssim |T - T_c| \lesssim 0.2$ °K. The T_c value from both sets of data agreed within experimental error, which was 0.2 mK for the coexistence curve and 0.5 mK for the K_T data. No significant difference was found for the values of the parameters as determined from either the liquid or the vapor side of the coexistence curve. Figure 2 shows a plot of $(\rho_L - \rho_c)$ versus $T_c - T$. We obtained

$$\begin{aligned} T_c &= 3.3105 \pm 0.0002 \text{ °K}, \\ \beta &= 0.361 \pm 0.005, \quad B = 1.31 \\ \gamma &= 1.18 \pm 0.08, \quad \Gamma = 2.48 \times 10^{-4} \text{ Torr}^{-1}, \\ \rho_c &= 0.04145 \pm 0.0002 \text{ g/cm}^3. \end{aligned}$$

The quality of the fit is significantly affected if

TABLE I. The values of the liquid and vapor densities ρ_L and ρ_G on the coexistence curve and their average. Above T_c we tabulate ρ_{inf1} as defined in text, which is very close to ρ_c .

A. Isothermal data							
T (°K)	P (Torr)	ρ_L g/cm ³	ρ_G g/cm ³	$\frac{1}{2}(\rho_L + \rho_G)$	T (°K)	$P(\rho_c)$ (Torr)	ρ_{inf1} g/cm ³
3.04478	648.8	0.063218	0.019587	0.04141	3.31199	861.4	0.0415
3.19985	766.75	0.057353	0.025464	0.04141	3.31500	864.05	0.0415
3.24981	807.75	0.054214	0.028564	0.04139	3.32000	868.4	0.0414
3.27981	833.25	0.051437	0.031545	0.04149	3.33000	877.25	0.0416
3.29481	846.15	0.049324	0.033741	0.04154	3.34501	890.7	0.0415
3.30001	850.80	0.048134	0.034758	0.04145	3.36999	912.8	0.0416
3.30500	855.15	0.046782	0.036120	0.04145	3.40000	940.0	0.0414
3.30801	857.80	0.045309	0.037642	0.04147	3.44369	979.35	0.0417
3.31000	859.7	0.043691	0.039215	0.04145			
B. Isobaric data							
P (Torr)	T (°K)	ρ_L g/cm ³	ρ_G g/cm ³	$\frac{1}{2}(\rho_L + \rho_G)$	P (Torr)	T (°K)	ρ_{inf1} g/cm ³
763.9	3.19616	0.057533	0.25342	0.04144	860.8	3.31140	0.0415
796.6	3.23627	0.055216	0.027688	0.04145	862.8	3.31360	0.0414
824.2	3.26910	0.052592	0.030332	0.04146	864.8	3.31590	0.0414
836.8	3.28374	0.050941	0.031986	0.04146	866.8	3.31824	0.0414
848.5	3.29737	0.048778	0.034242	0.04151	871.8	3.32396	0.0414
851.8	3.30116	0.047927	0.034965	0.04145	884.4	3.33791	0.0415
854.3	3.30400	0.047180	0.035758	0.04147	904.5	3.36057	0.0414
856.8	3.30685	0.046094	0.036675	0.04138	932.1	3.39131	0.0415
858.8	3.30910	0.0446	0.0383	0.04145	982.0	3.44659	0.0415

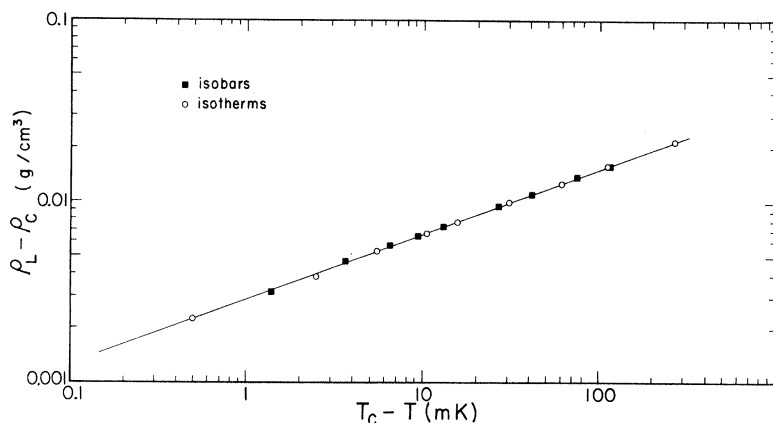


FIG. 2. Plot of the densities of liquid at the coexistence curve, expressed as $(\rho_L - \rho_c)$ versus $(T_c - T)$. Points for the vapor phase $(\rho_c - \rho_g)$ versus $(T_c - T)$, which are indistinguishable from the $(\rho_L - \rho_c)$ plot, are omitted from the graph.

the critical parameters are changed more than the indicated uncertainties. As pointed out before, the uncertainties of the absolute values of T_c and ρ_c are about ± 0.5 mK and 2.5×10^{-4} g/cm³, respectively. By an interpolation procedure between the isobars, we then obtain, including the hydrostatic correction, $P_c = 860.5 \pm 0.3$ Torr.

From the isobaric data we obtain the thermal expansion coefficient at the critical density for the various isobars. A logarithmic plot versus t yields $\gamma_P = 1.18 \pm 0.08$ and $\Gamma = 0.218$ °K⁻¹, in good agreement with previous work.⁷

As will be seen later, $(\partial P / \partial T)_\rho$ only changes about 2% for the range $T - T_c < 0.1$ °K, and hence can be approximated as a constant. Then, according to Eq. (16), we should have

$$\gamma_P = \gamma, \quad \Gamma_P = \left(\frac{\partial P}{\partial T} \right)_{\rho_c} \Gamma. \quad (24)$$

This relation is indeed satisfied by the experiment, confirming again the internal consistency of the data.

From a plot of $\Delta\mu$ versus $\rho - \rho_c$ in the one-phase region below T_c , we note the expected symmetry between the vapor and the liquid side. The derivatives $(\partial\rho/\partial\mu)_T = \rho^2 k_T$ on the coexistence curve are hence closely the same. A plot of $\partial\rho/\partial\mu$ on both sides of the coexistence curve versus T is shown in Fig. 3 and gives $\gamma' = 1.12 \pm 0.08$ and $\Gamma' = 6.9 \times 10^{-5}$ Torr⁻¹. We note from Fig. 3 that there is a tendency for γ' to be smaller than γ , although the extreme values, as determined by the experimental uncertainties, overlap. These results are in agreement with the findings of Chase and Zimmerman.⁹

The critical parameters are compared in Table II with those obtained in previous work. There is a disagreement in T_c and P_c with the earlier results⁷ of the cell 1 cm high by amounts that are somewhat outside the experimental uncertainty; this is not understood.

B. Critical Isobar and Isotherm

Although these curves were not measured directly, they were derived by a graphical interpolation technique suggested by Coopersmith.³¹ In the case of the isobars, for example, the method consists in plotting these curves with their inflection points (for $T > T_c$) and coexistence region ($T < T_c$) coincident, as shown in Fig. 4. The density values for each isobar were read off at constant-temperature intervals and were used to construct Fig. 5.

Using the values of T_c and P_c obtained before, the critical isobar was then plotted from Fig. 5.

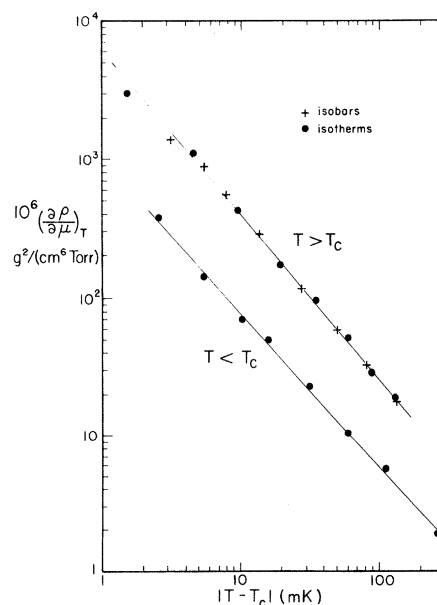


FIG. 3. Compressibilities $\rho^2 k_T = (\partial\rho/\partial\mu)_T$ from isotherms (open circles) and $\rho^2 k_T = \rho(\partial\rho/\partial T)_P (\partial T/\partial P)_{\rho_c}$ from isobars (black circles) along the isopycncnal ($t > 0$). Points on this latter curve represent the average for both liquid and vapor.

TABLE II. Critical parameters and properties of He³. [For the definition of the symbols, see Eqs. (1) – (9).]

Reference	β	δ	γ	γ'	π
this work	0.361	4.23	1.18 ^a	1.12 ^a	$\begin{cases} 4.21 (\rho > \rho_c) \\ 4.35 (\rho < \rho_c) \end{cases}$
Ref. 7	0.360		1.20		$\begin{cases} 3.9 (\rho > \rho_c) \\ 3.7 (\rho < \rho_c) \end{cases}$
Ref. 9	0.362	$\begin{cases} 3.97 (\rho > \rho_c) \\ 4.27 (\rho < \rho_c) \end{cases}$	1.19	1.08	
Ref. 12	0.48	3.4			
	B	∇	Γ	Γ'	π
this work	1.31	2.77	2.48×10^{-4}	6.9×10^{-5}	$\begin{cases} 0.73 (\rho > \rho_c) \\ 1.00 (\rho < \rho_c) \end{cases}$
Ref. 7	1.31				
Ref. 9	1.32				
	T_c	P_c	ρ_c	$\frac{dP}{dT}(T_c, P_c)$	
	(°K)	(Torr)	(g/cm ³)	(Torr)K ⁻¹	
this work	3.3105	860.5	0.04145	882	
Ref. 7	3.3095	861.8	0.04134		
Ref. 9	3.3094		0.0413		
Ref. 12	3.324	873	0.0418		

^aFrom the fit to the equation proposed by Missoni *et al.*, Ref. 5, we use $\gamma = \gamma' = 1.17$.

Using Eq. (6), the values of the exponents were then obtained for $|\Delta\rho| \leq 0.25$:

$$\rho > \rho_c, \quad \pi_+ = 4.21 \pm 0.1, \quad \Pi_+ = 0.73,$$

$$\rho < \rho_c, \quad \pi_- = 4.35 \pm 0.1, \quad \Pi_- = 1.00.$$

To give an idea of the change in the π 's when a slightly different value of P_c was chosen, we plotted isobars on both sides of the critical isobar, and derived the effective indices, as shown in

Table III. We see that a change of P_c by 0.2 Torr would cause a change in the π 's by about 0.08. The π_- values, however, were always found to be consistently higher than those for π_+ , showing the expected departure from antisymmetry in the isobars, when T and ρ are chosen to be conjugate variables.

Similarly to the above procedure, we plot a compressed representation of the isotherms as

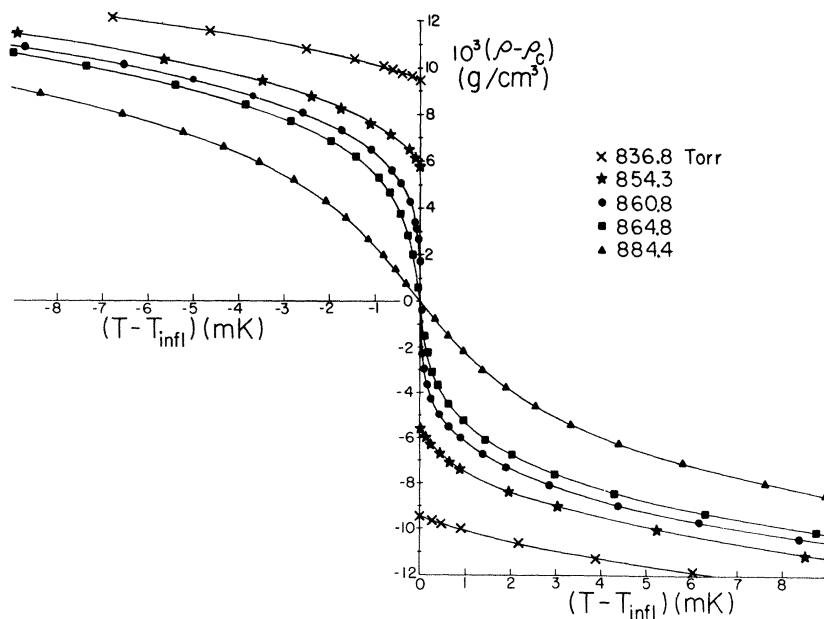


FIG. 4. Compressed plot of five representative isobars as $(\rho - \rho_c)$ versus $(T - T_c)$.

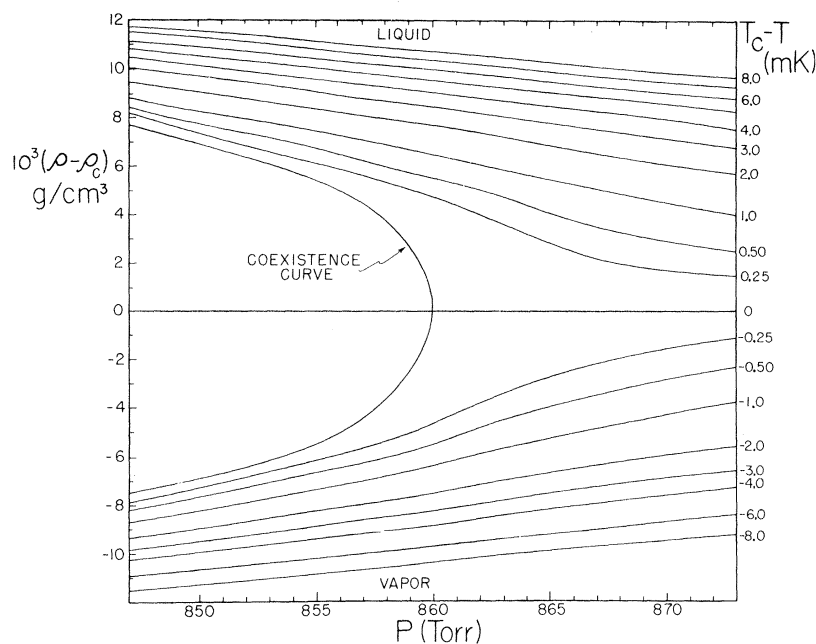


FIG. 5. Plot of $(\rho - \rho_c)$ versus P for a family of curves at constant $T - T_c$, as constructed from all the available isobars, represented as shown in Fig. 4.

$(\rho - \rho_c)$ versus $(P - P_c)$ (Fig. 6) and construct Fig. 7 which supplies $(\rho - \rho_c)$ for constant pressure intervals as a function of T . At $T = T_c$, we obtain the critical isotherm, and from a logarithmic plot of $P - P_c$ versus $\rho - \rho_c$, we obtain

$$\rho > \rho_c, \quad \delta_+ = 4.20 \pm 0.1, \quad \nabla_+ = 2.97,$$

$$\rho < \rho_c, \quad \delta_- = 4.06 \pm 0.1, \quad \nabla_- = 1.85.$$

A change of T_c by 0.2 mK causes a shift in δ by about 0.06. Furthermore, we find $\delta_+ = \pi_+$ within

TABLE III. Variation of the critical exponents δ and π of the critical isobar ($T - T_c \propto |\rho - \rho_c|^{\pi}$) and isotherm ($P - P_c \propto |\rho - \rho_c|^{\delta}$) for different choices of T_c , as obtained from logarithmic plots of $(T - T_c)$ versus $(\rho - \rho_c)$ (taken from Fig. 5) and from $(P - P_c)$ versus $(\rho - \rho_c)$ taken from Fig. 7. The hydrostatic pressure correction has not been applied to P_c .

		P (Torr)	π ($\rho < \rho_c$)	π ($\rho > \rho_c$)
P_c	→	859.5	4.56	4.36
		859.75	4.46	4.28
		860	4.35	4.21
		860.25	4.24	4.13
		860.5	4.14	4.06
		T (°K)	δ ($\rho < \rho_c$)	δ ($\rho > \rho_c$)
T_c	→	3.3101	4.17	4.37
		3.3103	4.11	4.27
		3.3105	4.06	4.20
		3.3107	4.00	4.12
		3.3109	3.94	4.04

experimental error, as expected from the theory of Griffiths.¹⁸ For the vapor phase, we find a tendency for π_- to be larger than δ_- by an amount slightly beyond the combined uncertainties. According to the scaling ideas, one should have $\pi = \delta$ on both liquid and vapor sides. It is possible that in the experiment, the asymptotic region where this equality holds has not been reached; this may account for the marginal discrepancy.

C. Critical Isochore

The P -versus- T data along the critical isochore were taken to determine $(\partial P / \partial T)_\rho$ and to check for the possibility of a logarithmic singularity in $(\partial^2 P / \partial T^2)_{\rho_c}$ and $(\partial^2 \mu / \partial T^2)_{\rho_c}$. Such measurements have also been made for He⁴ by Kierstead.³² The derivative was obtained from a subtraction between adjacent (P, T) pairs on this isochore, and the results are shown in Fig. 8. We note that $d^2 P / dT^2 > 0$ and that it appears to go through a singularity at T_c , although the scatter prevents a precise study of this.

The thermodynamic expression to be used is

$$C_v = TV \frac{d^2 P}{dT^2} - T \frac{d^2 \mu}{dT^2} \quad \text{coexistence}$$

$$= TV \left(\frac{\partial^2 P}{\partial T^2} \right)_{\rho_c} - T \left(\frac{\partial^2 \mu}{\partial T^2} \right)_{\rho_c}, \quad T > T_c. \quad (25)$$

The results of Moldover,¹¹ which show an almost logarithmic singularity in C_v near T_c , require then that there be a singularity in either $d^2 P / dT^2$ or $d^2 \mu / dT^2$ or both. This has been discussed by Missoni *et al.*⁵ among others.¹¹ From an analysis

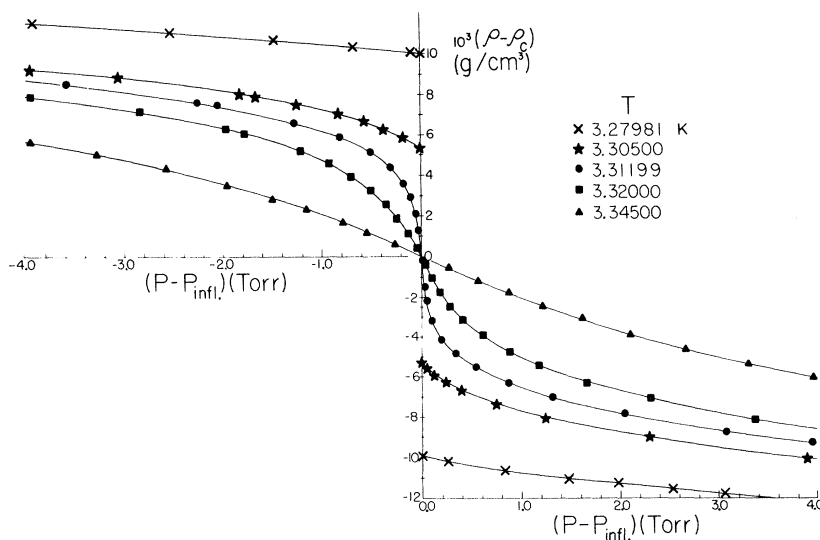


FIG. 6. Compressed plot of five representative isotherms as $(\rho - \rho_c)$ versus $(P - P_c)$.

of data on He⁴, Ar, and steam, these authors⁵ conclude that from the meager amount of data available there is no experimental evidence for a rapid change or divergence of $d^2\mu/dT^2$ in the two-phase region. Integration of Eq. (25) gives for $\rho = \rho_c$

$$\left(\frac{\partial P}{\partial T}\right)_\rho(\rho_c, T) + \frac{1}{V_c} \int_{T_c}^T \frac{C_v dT}{T} = \left(\frac{\partial P}{\partial T}\right)_\rho(\rho_c, T_c) - \frac{1}{V_c} \int_{T_c}^T \frac{d^2\mu}{dT^2} dT. \quad (26)$$

Using, in this equation, the numerically integrated results by Moldover, we obtain to good approximation, as shown in Fig. 8:

$$\frac{1}{P_c V_c} \int_{T_c}^T \left(\frac{d^2\mu}{dT^2}\right) dT = -0.22(T - T_c), \quad |T - T_c| \leq 0.1. \quad (27)$$

Hence there appears to be no singularity in $d^2\mu/dT^2$ in the critical region. More precise measurements of dP/dT are necessary, however, to make sure that with a higher resolution no singularity can be detected.

D. Fit of the Isotherms to the Expression of Missoni *et al.*

In general, the unsmoothed $\Delta\mu$ -versus- $\Delta\rho$ plot was so close to being antisymmetric around ρ_c for $|\Delta\rho| \lesssim 0.25$ and $|t| \lesssim 0.03$ that an average curve $\Delta\mu$ versus $\Delta\rho$ represented well the behavior on either side of ρ_c or of the coexistence curve within the uncertainty of the original data. We applied a least-squares fit to Eqs. (18) and (20) using 150 such values taken from eight isotherms ($3.2948 \leq T \leq 3.3300$ °K). Starting from values of ρ_c , x_0 , β ,

and T_c as determined previously, the procedure was to iterate on δ while finding E_1 and E_2 . We also applied small changes to ρ_c , x_0 , β , and T_c within the limits of our experimental errors that would result in only small changes in E_1 , E_2 , and δ . We were able to represent our data with the values $x_0 = 0.475$, $E_1 = 2.53$, $E_2 = 0.44$, and $\delta = 4.23$ for the optimum fit. These numbers are similar to those found for He⁴, Xe, and CO₂, except for δ , which we believe is definitely less than the value of about 4.5 given for these gases. From the experience gained in the fitting of experiment to theory, δ in He³ may not change by over 0.10 without seriously affecting the quality of the fit. Any change in δ will cause a corresponding change in E_1 and E_2 . A plot of the departure from the theoretical curve, expressed as $\Delta h(x)/h(x)$ versus x is shown in Fig. 9. In this plot, additional isotherms, that were not used for obtaining the fit, are shown. They are consistent with the others. The scatter appears to be almost random around the zero value for $\Delta h(x)/h(x)$, with a slight tendency for the departure to increase with $(x_0 + x)/x_0$. It should be pointed out, however, that it would be easy to obtain a truly random scatter around the horizontal zero axis by assuming an individual variation of the effective value of ρ_c for the various isotherms by at most 0.2%, as due to inevitable small shifts, uncertainties in the analysis, etc. This error is entirely within the limits of our quoted uncertainty. For instance, a change of the density by 0.2% causes $\Delta h(x)/h(x)$ to change between about 2% and 9% over the range of the values of $\log(x + x_0)/x_0$. From our reanalysis of the data²⁴ on He⁴, and a representation into a plot similar to that in Fig. 9, we conclude that the scatter of the data as fitted to theory is comparable for both isotopes.

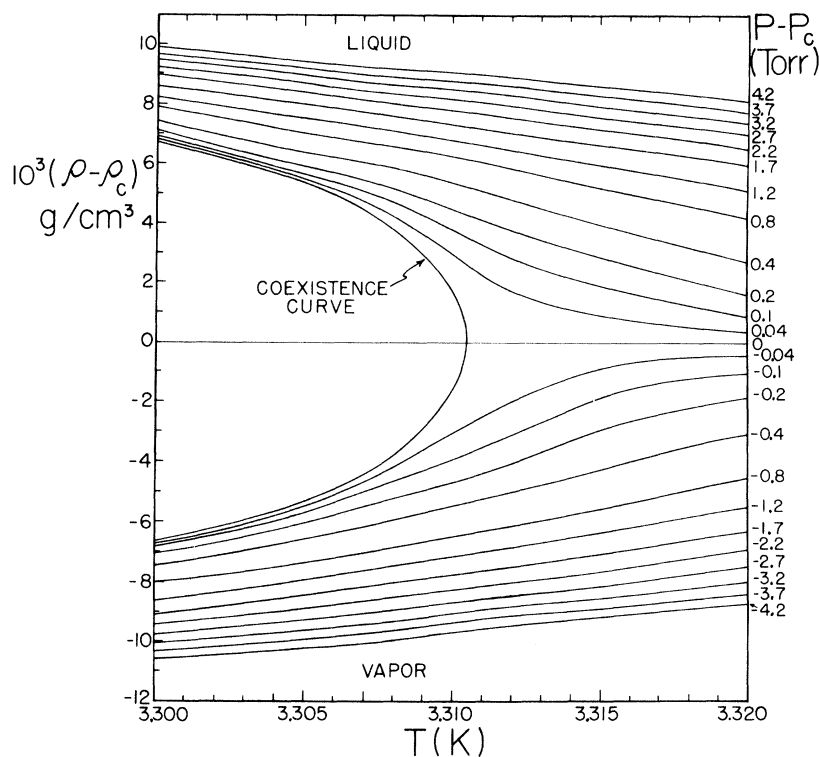


FIG. 7. Plot of $\rho - \rho_c$ versus T for a family of curves with constant $(P - P_c)$ for all available isobars represented in the way shown in Fig. 6.

Using the maximum allowed values for β and δ , we obtain $\beta(\delta + 1) = 1.95$. Therefore Griffiths's inequality [Eq. (12)] is satisfied provided $\alpha' \geq 0.05$. This is to be related to a graphical analysis of specific-heat results, which indicates that α' cannot exceed about 0.1. Hence it appears that for He^3 $0.05 < \alpha < 0.1$. As a check, we have integrated the chemical potential along the critical isotherm con-

structed from Fig. 7, Table IV, and obtained $\delta(\rho > \rho_c) = 4.20 \pm 0.10$ and $\delta(\rho < \rho_c) = 4.22 \pm 0.10$, which are the same within the combined uncertainties, and consistent with the results from the fitting procedure to Eqs. (20) and (21) as described above.

VI. EXPERIMENTS WITH He^3 (10 ppm He^4)

We have also conducted a less extensive research

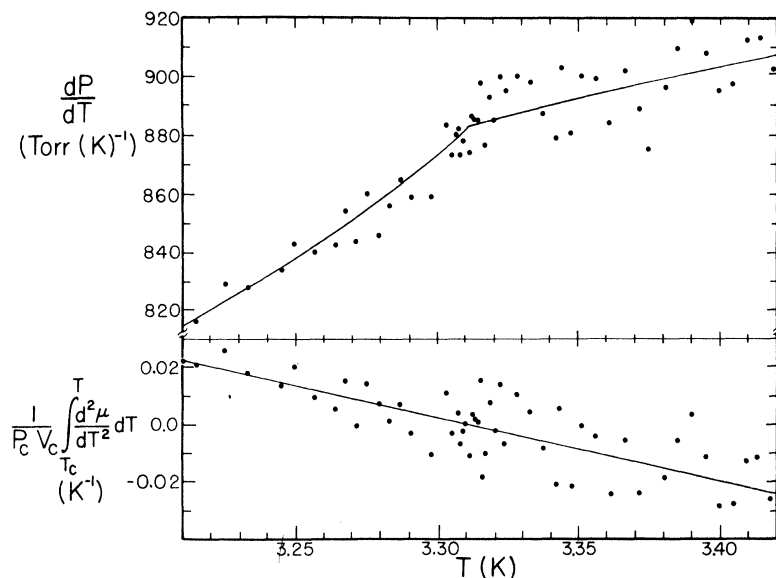


FIG. 8. Top part: plot of the derivative of the vapor-pressure curve dP/dT versus T . Above T_c , plot of $(\partial P/\partial T)_{\rho=\rho_c}$ versus T . Solid line in the top diagram is calculated using Eq. (26) with the specific heat of Moldover, using the results of Eq. (27) and normalizing the curve to $dP/dT = 882$ Torr (K^{-1}) at the critical point. Solid line on the bottom part curve is the best linear fit to the experimental points. Bottom part: plot of $(P_c V_c)^{-1} \int_{T_c}^T \partial^2 \mu / \partial T^2 dT$ versus T .

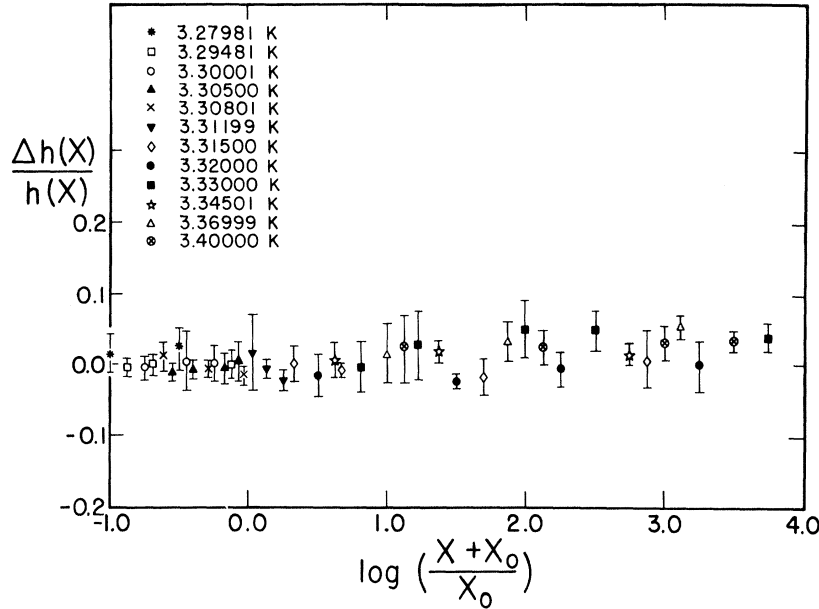


FIG. 9. Relative deviation, $\Delta h(x)/h(x) = [h_{\text{expt}} - h_{\text{fitted}}(x)]/h(x)$ versus $\log[(x + x_0)/x_0]$. The vertical error bars represent the experimental uncertainties. Although 150 data points were involved in obtaining the fit, only 41 were plotted here to avoid overcrowding, especially near $\log[(x + x_0)/x_0] = 0$. These points are a random selection and representative of the fit to the scaling equation of Missoni *et al.*

with purer He³ than described above, in order to ascertain whether some of the properties in the immediate vicinity of T_c were substantially modified by small He⁴ impurities. A series of isotherms at the same temperatures as in Table I, and the critical isochore (P, T) were recorded. These results have somewhat more scatter, due to a slight instability of the tunnel diode oscillator. Their analysis, carried out in the same way as described before, omitting the fit to the theory of Missoni

et al.,⁵ does not give substantially different results. We find $T_c = 3.3098^\circ\text{K}$, $\rho_c = 0.04137\text{ g/cm}^3$, $P_c = 860.2\text{ Torr}$, $(dP/dT)(T_c, \rho_c) = 880\text{ Torr/K}$, $\beta = 0.361 \pm 0.005$, $\gamma = 1.19 \pm 0.10$, and $\delta = 4.20 \pm 0.10$.

One expects the critical temperature of He³ (250 ppm He⁴) to lie above the critical temperature for pure He³ by approximately $\Delta T_c = 2.5 \times 10^{-4} [T_c(\text{He}^4) - T_c(\text{He}^3)] \approx 5 \times 10^{-4}^\circ\text{K}$. Since the two samples were measured in two different series of experiments, with two different temperature calibrations, such a small

TABLE IV. Critical isotherm, as obtained by graphical construction from Fig. 7.

$(10^{-1})\Delta\rho$	$\rho > \rho_c$ $P - P_c$ (Torr)	$\frac{10^{-3}(\mu - \mu_c)}{P_c V_c}$	$-10^{-1}\Delta\rho$	$\rho < \rho_c$ $-(P - P_c)$ (Torr)	$-\frac{10^{-3}(\mu - \mu_c)}{P_c V_c}$
1.0471	0.2	0.21556	0.90512	0.1	0.11921
1.1617	0.3	0.32029	1.0982	0.2	0.24856
1.2474	0.4	0.42401	1.2116	0.3	0.38007
1.3801	0.6	0.62932	1.2985	0.4	0.51307
1.4791	0.8	0.83278	1.4396	0.6	0.78263
1.5539	1.0	1.0346	1.5470	0.8	1.5607
1.6962	1.5	1.5345	1.6363	1.0	1.3327
1.8169	2.0	2.0291	1.8064	1.5	2.0355
1.9207	2.5	2.5188	1.9343	2.0	2.7510
1.9979	3.0	3.0049	2.0429	2.5	3.4769
2.0703	3.5	3.4881	2.1394	3.0	4.2121
2.1415	4.0	3.9683	2.2203	3.5	4.9558
2.3623	6.0	5.8644	2.2927	4.0	5.7065
2.6518	10.0	9.5792	2.5485	6.0	8.7792
2.8690	14.0	13.223	2.7415	8.0	11.943
3.0814	19.0	17.702	3.0359	12.0	18.491
3.2551	24.0	22.116	3.2724	16.0	25.290
3.4011	29.0	26.478	3.4679	20.0	32.307
3.5278	34.0	30.795			

shift is within the uncertainty of the absolute temperature calibration, which is about 0.5 mK for each series of experiments.

VII. CONCLUSIONS

From a detailed study of the equation of state of He³ near the critical point, we draw the following conclusions. (a) The scaling-law approximation that uses power laws with critical exponents is well justified by experimental evidence for He³, at least for the density range $\Delta\rho \leq 0.25$. (b) The relations between the various critical exponents are all satisfied by the experiments, provided the exponent for the specific heat, α' , is larger than 0.05, which is not inconsistent with a cursory graphical analysis of Moldover's data. (c) The exponent γ is found to be slightly larger than γ' , but their combined uncertainties are such that one can speak of an average value of about 1.17, representative for regions both above and below T_c . (d) A comparison of the critical exponents for the critical isotherm and isobar where (ρ, P) and (ρ, T) are, respectively, the variables shows that on the liquid side $\pi = \delta$. On the vapor side there is a tendency of π to be larger than δ , but the difference is marginal. The equality for the liquid is in agreement with the prediction by Griffiths,¹⁸ while there is no such prediction for the vapor side. (e) Combination of the P, T measurements along the critical isochore with the specific-heat measurements of Moldover show that within the experimental scatter,

$$\frac{1}{P_c V_c} \frac{d^2 \mu}{dT^2} = -0.22 (\text{K})^{-2} \text{ for } |t| \lesssim 0.03,$$

which is the experimental temperature range. Hence no singularity could be detected. However, since such a singularity, if any, would have only a small effect on the vapor-pressure curve, pressure measurements with considerably higher resolution

would have to be carried out to obtain complete certainty. The value of dP/dT at the critical point is $882 \pm 5 \text{ Torr (K)}^{-1}$. (f) There is good agreement in the critical exponents with those obtained in previous measurements on He³, except for δ which is found to be larger in the present research. The critical exponents are also in good agreement with those for He⁴, Xe, and CO₂, with the exception again of δ , which is slightly smaller for He³. Thus, on the whole, quantum effects on the exponents for the helium isotopes appear to be insignificant. (g) A fit of the isotherm data, expressed as $\Delta\mu$ versus $\Delta\rho$ to the proposed equation of state by Missoni *et al.* is very satisfactory, as indicated by the scatter in Fig. 9 which shows the departures from this fit. In this theory, $\gamma = \gamma'$, but as mentioned before, the direct analysis of the compressibility data indicates a tendency for γ' to be smaller than γ . The parameters E_1 , E_2 , and δ obtained from the fit, are reasonably consistent with those for He⁴, CO₂, and Xe. (h) The critical isotherm, expressed as $\Delta\mu$ versus $\Delta\rho$, is antisymmetric within experimental error for $|\Delta\rho| \lesssim 0.25$. For $\Delta\rho = 0.35$, we have

$$\left[|\Delta\mu(\rho < \rho_c)| - |\Delta\mu(\rho > \rho_c)| \right] / |\langle \Delta\mu \rangle_{av}| \approx 0.11.$$

An analysis into an antisymmetric and a symmetric term as suggested by Griffiths¹⁸ is too uncertain for these data and is being carried out at present for data extending to density values up to about $|\Delta\rho| \approx 0.6$. These results will be reported elsewhere.

ACKNOWLEDGMENTS

The authors are grateful to Dr. M. Missoni and to Professor R. B. Griffiths for several stimulating discussions and useful suggestions, and also for their constructive comments on the manuscript.

*Research supported by a National Science Foundation grant.

¹See for instance L. P. Kadanoff, D. Aspnes, W. Goetze, D. Hamblen, R. Hecht, J. Kane, E. A. S. Lewis, V. V. Palciauskas, M. Rayl, and J. Swift, *Rev. Mod. Phys.* **39**, 395 (1967); see also *Critical Phenomena*, edited by M. S. Green and J. V. Sengers, National Bureau of Standards, Miscellaneous Publication No. 273 (GPO, Washington, D. C., 1966).

²B. Widom, *J. Chem. Phys.* **43**, 3898 (1965).

³R. B. Griffiths, *Phys. Rev.* **158**, 176 (1967).

⁴M. Vicentini-Missoni, J. M. H. Levelt Sengers, and M. S. Green, *Phys. Rev. Letters* **22**, 389 (1969).

⁵M. Vicentini-Missoni, J. M. H. Levelt Sengers, and M. S. Green, *J. Res. Natl. Bur. Std. (U.S.)* **73A**, 563 (1969).

⁶P. Schofield, J. D. Litster, and J. Ho, *Phys. Rev. Letters* **23**, 1098 (1969).

⁷W. Bendiner, D. Elwell, and H. Meyer, *Phys. Letters*

26A, 421 (1968).

⁸E. C. Kerr and R. H. Sherman, *Proceedings of the Eleventh International Conference on Low Temperature Physics, St. Andrews, Scotland, 1968*, edited by J. F. Allen, D. M. Finlayson, and D. M. McCall (University of St. Andrews Printing Department, St. Andrews, Scotland, 1969), Vol. 1, p. 236.

⁹C. E. Chase and G. Zimmerman, in Ref. 8, p. 224.

¹⁰M. Moldover and W. Little, in *Critical Phenomena*, p. 79.

¹¹M. Moldover, thesis, Stanford University, 1967 (unpublished).

¹²R. H. Sherman, *Phys. Rev. Letters* **15**, 141 (1965).

¹³R. H. Sherman, in Ref. 10, p. 7.

¹⁴G. Zimmerman and C. Chase, *Phys. Rev. Letters* **19**, 151 (1967).

¹⁵J. Ho and J. D. Litster (unpublished).

¹⁶R. B. Griffiths (private communication).

¹⁷M. E. Fisher, in Ref. 10, p. 21; *J. Math. Phys.* **5**,

944 (1964).

¹⁸R. B. Griffiths, *J. Chem. Phys.* **43**, 1958 (1965).¹⁹R. B. Griffiths, *Phys. Rev. Letters* **14**, 623 (1965).²⁰G. S. Rusbrooke, *J. Chem. Phys.* **39**, 842 (1963).²¹M. J. Buckingham (unpublished).²²C. Boghosian, H. Meyer, and J. E. Rives, *Phys. Rev.* **146**, 110 (1966).²³H. Van Dijk, M. Durieux, J. R. Clement, and J. K. Logan, *Physica* **24**, S129 (1954).²⁴P. Roach, *Phys. Rev.* **170**, 213 (1968).²⁵D. Elwell and H. Meyer, *Phys. Rev.* **164**, 245 (1967); D. Elwell, thesis, Duke University, 1967 (unpublished).²⁶O. V. Lounasmaa, *Cryogenics* **1**, 1 (1961).²⁷R. H. Sherman and F. J. Edeskuty, *Ann. Phys. (N. Y.)* **9**, 522 (1960).²⁸E. C. Kerr and R. D. Taylor, *Ann. Phys. (N. Y.)* **20**, 450 (1962).²⁹Interestingly, the ratio $\bar{\rho}(T=0)/\rho_c$ is 0.98 for He³, while for He⁴ it is 0.145/(2×0.069)=1.05, where we use the value of the density ρ_L ($T=0$) obtained by K. R. Atkins and M. H. Edwards [*Phys. Rev.* **97**, 1429 (1955)] and ρ_c obtained by Roach, Ref. 24.³⁰B. Widom, *J. Chem. Phys.* **43**, 3898 (1965), p. 3901.³¹M. Coopersmith, *Phys. Rev. Letters* **20**, 432 (1968).³²H. Kierstead (private communication).

Kinetic Theory of a Weakly Coupled Fluid*

Dieter Forster[†] and P. C. Martin*Lyman Laboratory of Physics, Harvard University, Cambridge, Massachusetts 02138*

(Received 6 April 1970)

Virtually all measurable properties of a classical fluid may be determined from the expectation value of the phase-space density operator $f(\vec{r}\vec{p}t) = \sum_{\alpha} \delta(\vec{r} - \vec{r}^{\alpha}(t)) \delta(\vec{p} - \vec{p}^{\alpha}(t))$, and the phase-space density correlation function $\langle f(\vec{r}\vec{p}t)f(\vec{r}'\vec{p}'t') \rangle - \langle f(\vec{r}\vec{p}t) \rangle \langle f(\vec{r}'\vec{p}'t') \rangle$, a matrix with indices $(\vec{r}\vec{p}t)$. Systematic procedures for approximating this matrix, unhindered by secular effects, are always based on approximations to its inverse. For a weakly coupled fluid, the inverse can be expanded in powers of λ , the ratio of potential to kinetic energy. The leading term in this expansion gives rise to a Vlasov equation for the phase-space correlation function. The next term is the first that includes collisions, and results in relaxation towards equilibrium. This paper is concerned with the detailed study of the resulting fundamental nontrivial approximation. It is not Markovian and is perfectly reversible. Although the approximation is complicated, it is tractable analytically in various limits, and numerically for all wavelengths and frequencies. In this paper, only the behavior in certain limits is evaluated. Particular attention is directed toward its contractions – the density correlation function, which is measured by inelastic neutron and light scattering, and the momentum correlation function. Calculation of the former at long wavelengths corroborates the Landau-Placzek expression for light scattering, and therefore demonstrates that the kinetic equation predicts hydrodynamic behavior at long times. Since the correlation function is correct to order λ^2 , it has, in contrast to a solution to the Boltzmann equation, the correct long-wavelength velocity of sound, $c^2 = (d\bar{p}/dmn)_{\bar{s}} \neq \frac{5}{3} k_B T/m$. It also predicts different transport coefficients than those deduced from a Boltzmann equation. These include a nonvanishing bulk viscosity. The transport coefficients reduce to those derived from the Boltzmann equation at low densities. Some aspects of the short-time behavior are also discussed.

I. INTRODUCTION

The measurable properties of a system of classical spinless particles are properties which can be constructed from observables formed from the field

$$f(\vec{r}\vec{p}t) = \sum_{\alpha} \delta(\vec{r} - \vec{r}^{\alpha}(t)) \delta(\vec{p} - \vec{p}^{\alpha}(t)),$$

in which α extends over all the indistinguishable particles in the system. Thus, a study of the dynamics of such a system is an investigation of $\langle f(\vec{r}\vec{p}t) \rangle$, $\langle f(\vec{r}\vec{p}t)f(\vec{r}'\vec{p}'t') \rangle$, etc. Fundamentally, the equation which governs these products is the Liouville equation, and the determination of these

correlations for an arbitrary state requires a specification of the initial conditions of all products $\langle f(\vec{r}\vec{p}t) \dots \rangle$, since they are all necessary to characterize an arbitrary state. It has been recognized for some time, however, that an important class of problems can be understood from a knowledge of $\langle f(\vec{r}\vec{p}t)f(\vec{r}'\vec{p}'t') \rangle_{\text{eq}}$ in an equilibrium ensemble. In particular, because of the connection between fluctuations and linear response, the equilibrium fluctuation function

$$S(\vec{r} - \vec{r}', t - t'; \vec{p}\vec{p}') = \langle (f(\vec{r}\vec{p}t) - \langle f(\vec{r}\vec{p}t) \rangle_{\text{eq}}) \times (f(\vec{r}'\vec{p}'t') - \langle f(\vec{r}'\vec{p}'t') \rangle_{\text{eq}}) \rangle_{\text{eq}}$$